Allosteric Kissing Complex-Based Electrochemical Biosensor for Sensitive, Regenerative and Versatile Detection of Proteins

Mingsha Zhao, Shanshan Zhang, Zhiqiang Chen, Changzhi Zhao, Li Wang, Shufeng Liu

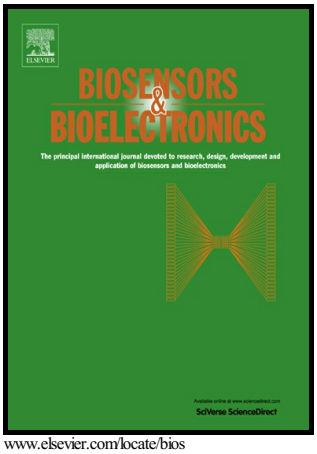

www.elsevier.com/locate/bios

PII: S0956-5663(18)30021-6
DOI: https://doi.org/10.1016/j.bios.2018.01.015
Reference: BIOS10208

To appear in: *Biosensors and Bioelectronic*

Received date: 6 November 2017
Revised date: 4 January 2018
Accepted date: 8 January 2018

Cite this article as: Mingsha Zhao, Shanshan Zhang, Zhiqiang Chen, Changzhi Zhao, Li Wang and Shufeng Liu, Allosteric Kissing Complex-Based Electrochemical Biosensor for Sensitive, Regenerative and Versatile Detection of Proteins, *Biosensors and Bioelectronic,* https://doi.org/10.1016/j.bios.2018.01.015

Allosteric Kissing Complex-Based Electrochemical Biosensor for Sensitive, Regenerative and Versatile Detection of Proteins

Mingsha Zhao, Shanshan Zhang, Zhiqiang Chen, Changzhi Zhao, Li Wang, and Shufeng Liu*

Key Laboratory of Sensor Analysis of Tumor Marker, Ministry of Education, College of Chemistry and Molecular Engineering, Qingdao University of Science and Technology, No.53, Rd. Zhengzhou, Qingdao, Shandong 266042, China.

*Corresponding author. Tel.&Fax. 86-532-84022681. E-mail address: sliu@qust.edu.cn

Abstract

Herein, an allosteric kissing complex-based electrochemical biosensor was ingeniously proposed for the simple, sensitive, regenerative and versatile detection of proteins. Two hairpins (Hp1 and Hp2) were designed and the Hp1 was immobilized on the electrode surface, which could form a kissing complex with Hp2 through the apical loop-loop or kissing interaction of the RNA-RNA base sequences. The Hp2 possesses the appended single-stranded tails on each end, which hybridize with the recognition element-conjugated DNA strands to construct a protein responsive switch of Hp2 scaffold. After kissing complex formation between the Hp2 scaffold and the immobilized Hp1, the streptavidin-labeled alkaline phosphatase (SA-ALP) can be introduced onto the electrode surface for the generation of electrochemical signal. In the presence of target protein, its binding to the recognition elements linked onto the Hp2 scaffold endows the steric strain to open the Hp2 stem, propagated by the disruption of the kissing complex structure, resulting into a decreased electrochemical signal related with the protein quantification. Also, the Hp1 immobilized electrode can be directly regenerated after protein-induced kissing complex dissociation. The current kissing complex-based electrochemical biosensing strategy can be easily extended for the detection toward different protein targets of interest by simply changing the recognition elements conjugated onto the Hp2 scaffold. The sensitive and selective detection toward proteins could be achieved with the detection limits toward Anti-Dig antibody and thrombin of about 1 ng/mL and 10 pM, respectively. The developed kissing complex-based protein biosensing strategy should be a beneficial supplement in current biosensor field, providing a promising means for the applications in bioanalysis, disease diagnostics, and clinical biomedicine.

Keywords: Electrochemical biosensor; Protein detection; Kissing complex; Nucleic acid

1. Introduction

The development of simple, low cost and point-of-care approaches for the quantitative detection of protein biomarkers is highly pursued to accommodate the global health issue confronted especially in the developing world (Rifai et al., 2006; Chikkaveeraiah et al., 2012; Kosaka et al., 2014; Hanash et al., 2008; Rica and Stevens, 2012; Yetisen et al., 2013). Some routine methods toward protein analysis, for example enzyme-linked immunosorbent assays, western blots and polarization assays (Han et al., 2008; Bakalova et al., 2005; Lai et al., 2004; Jameson and Ross, 2010), are often confronted with expensive instruments or sophisticated operation processes, which limits the wide applications of these methods in routine clinical diagnosis. Also, among different available signal readout means, electrochemical detection shows the outstanding attributes in terms of its low cost, inherent signal stability and ease of calibration (Liu et al., 2015a; Ronkainen et al., 2010; Chen et al., 2014; Tang and Ma, 2017). Furthermore, it can be easily integrated with some miniaturized devices or lab-on-a-chip platforms, thus holding a promising potential for the fabrication of portable and point-of-care biosensor.

Recently, the nucleic acid-based protein conversion or detection strategies are especially intriguing for protein biosensor fabrication owing to the advantages of nucleic acid structure including its programmable base-pairings, ease of synthesis and modification, and facile grafting with the successive signal readout or amplification (Yang et al., 2016; Li et al., 2012; Zhang et al., 2015; Li et al., 2017; Jung and Ellington, 2014; Zhang et al., 2013; Mahshid et al., 2015). For example, the terminal protection strategy of DNA has been widely developed for protein analysis (Wu et al., 2009; Wang et al., 2015; Wang et al., 2013; Wu et al., 2011; Liu et al., 2015; Cao et al., 2012), which is based on the DNA degradation inhibition by nucleases after the protein binding with the small molecule moiety labeled on the DNA terminus, thus converting the binding event of small molecule with target protein into the presence of a specific DNA sequence. In such protein conversion strategy,

the use of specific nuclease is necessary. Also in order to avoid the undetermined effects of nuclease toward the succeeding operation, the additional deactivation treatment toward nuclease is usually conducted. The proximity-dependent immunoassay or aptasensor has also been widely proposed for protein detection, which is based on the simultaneous recognition of a target protein by a pair of affinity probes, inducing the oligonucleotide tails of the bound probes into close proximity for the promotion of ligation or hybridization (Hu et al., 2012; Zhang et al., 2007; Li et al., 2015; Fredriksson et al., 2002; Burbulis et al., 2005). It can simplify the detection procedures or easily couple with different nucleic acid amplification techniques, but it necessitates the relatively complex or delicate nucleic acid sequence optimization to alleviate the background response or avoid the possible false-positive signal. Inspired from many naturally occurring biorecognition systems, the development of artificial protein-responsive nucleic acid switch has become another research focus for biosensor fabrication. The sensing mechanism is usually operated based on the protein-induced conformation change of the designed nucleic acid skeleton that contains the protein recognition element or aptamer sequence (Ranallo et al., 2015; Ranallo et al., 2017; Vallée-Bélisle et al., 2012; Xiao et al., 2005). With the direct linking of signaling labels to such specific, binding-induced event, such conformation change after protein binding can be followed by the signal change, which can effectively avoid the inclusion of exogenous reagents or coupling to exogenous biochemical reactions. However, the sensitivity toward protein is often plagued with the relatively high background response and the compromised signal gain, which is limited to the conformation change size of the receptor to some extent. In this context, the development of simple, cost-effective and sensitive nucleic acid-based protein biosensing strategy would be of very importance for bioanalysis and disease diagnostics.

Herein, an allosteric kissing complex-based electrochemical biosensor for sensitive, versatile and regenerative protein detection was proposed for the first time. It takes advantage of a kissing complex that switches from the

associated to the detached status in the case of target protein. A kissing complex between two designed hairpins (Hp1 and Hp2 scaffold) was firstly formed on the electrode surface through the apical loop-loop or kissing interaction of the RNA-RNA base sequences. The stability of such so-called RNA-RNA kissing complex can be attributed to the Watson–Crick base pairs in the loop–loop helix and the stacking interactions at the junctions between the loop-loop module and the double-stranded stem of each hairpin partner (Durand et al., 2014; Chovelon et al., 2016; Zhang et al., 2016). Then, the streptavidin-labeled alkaline phosphatase (SA-ALP) was brought to the electrode for the generation of an electrochemical response (Carpini et al., 2004). The further protein binding with the recognition elements linked onto the Hp2 scaffold endowed the steric strain to shift the Hp2 conformation from a folded to an unfolded shape, propagated by the dissociation of kissing complex, resulting into a decreased electrochemical signal. Thus, protein recognition could be effectively quantified based on the electrochemical signal change before and after its binding.

2. Experimental section

2.1 Materials and chemicals.

Thrombin, sheep polyclonal anti-digoxigenin antibody (Anti-Dig antibody), mouse immunoglobin G (IgG), 6-mercaptohexanol (MCH), tris(2-carboxyethyl)phosphine hydrochloride (TCEP), and 1-Naphthyl phosphate (1-NP) were obtained from Sigma-Aldrich (St. Louis, MO, USA). Bovine serum albumin (BSA), α-Fetoprotein (AFP) and streptavidin-alkaline phosphatase (SA-ALP) were supplied by Dingguo Biotech Co., Ltd. (Beijing, China). All the HPLC-purified oligonucleotide sequences were purchased from Takara (Dalian, China) and listed in Table S1. Fetal calf serum was obtained from Sangon Biotech. Co., Ltd. (Shanghai, China). All other reagents were of analytical grade without further purification.

2.2 Immobilization of hairpin RNA (Hp1) on the Au electrode.

The gold electrode (2 mm diameter) was sequentially polished with 1.0, 0.3 and 0.05 μm alumina power, followed by ultrasonic cleaning in acetone

and water. Subsequently, the gold electrode was dipped in a freshly prepared piranha solution (a 3:1 v/v mixture of concentrated H_2SO_4 and 30% H_2O_2) for 5 min, and rinsed thoroughly with water. Then, it was electrochemically scanned by cycling the potential between -0.2 to +1.5 V in 0.5 M H_2SO_4 solution until the stable cyclic voltammogram was obtained. The pretreated gold electrode was immersed into a 1 μM thiolated Hp1 in 10 mM Tris-HCl buffer (0.3 M NaCl, 1mM EDTA, 10 mM TCEP, pH 7.4) for 3 h at room temperature. Afterward, the electrode was immersed into 1 mM MCH for 20 min to remove the possible nonspecific adsorption.

2.3 Kissing complex formation with the Hp2 scaffold.

The protein-responsive switch of Hp2 scaffold was firstly prepared by annealing the Hp2 with two Dig-labeled single-stranded DNA (Dig-S1 and Dig-S2. In the case for thrombin detection, the Dig was replaced by the aptamer sequence) with the same concentration in 20 mM Tris-HCl (pH 7.4, 0.1 M NaCl, 10 mM $MgCl_2$) at 37 ^oC for 2 h. Then the Hp1 immobilized electrode was immersed into the above mixed solution containing 1 μM Hp2 scaffold at 37 ^oC for 1 h to form a kissing complex on the electrode surface. The obtained electrode was further immersed into a 2% BSA solution for 30 min to block the possible nonspecific site.

2.4 Protein recognition.

The kissing complex modified electrode was incubated into the test solution containing different concentrations of Anti-Dig antibody or thrombin at 37 ^oC for 45 min. After that, 20 μL 5 μg/mL SA-ALP solution was added onto the electrode surface and incubated at 37 °C for 40 min.

2.5 Electrochemical measurement.

Differential pulse voltammetric (DPV) experiments were recorded in 100 mM Tris-HCl buffer (1 mM Mg^{2+}, pH 9.8) containing 4 mM 1-NP with the potential window from 0 V to 0.55 V, the pulse amplitude of 50 mV and the pulse period of 0.2 S. The electrochemical impedance spectra (EIS) were recorded in 10 mM $[Fe(CN)_6]^{3-/4-}$ and 1 mM KCl with the frequency range from 0.1 Hz to 10 kHz. Before measurements, the electrolyte solution should

be purged with nitrogen gas for about 30 min.

2.6 Polyacrylamide gel electrophoresis.

17.5% polyacrylamide hydrogel was prepared by mixing 3.5 mL 40% gel solution (39:1), 160 μL 50×TAE Buffer, 80 μL 10% APS, 4 μl TEMED and 4256 μL deionized water. The polyacrylamide gel electrophoresis (PAGE) was carried out in 1×TAE buffer at a constant voltage of 180 V for 3 min, and then at a constant voltage of 135V for about 90 min at room temperature, and then stained in ethidium bromide (EB) dye solution.

2.7 Apparatus.

The electrochemical measurements were operated on a CHI 660D electrochemical workstation (CH Instruments, Shanghai, China) by using a conventional three-electrode system consisted of a gold electrode as the working electrode, a platinum wire as the auxiliary electrode, and a Ag/AgCl reference electrode. The gels were scanned using an FR-980A gel image analysis system (Shanghai, China).

3. Results and discussion

3.1 Design principle of the kissing complex-based electrochemical protein biosensor.

The fabrication of the allosteric kissing complex-based electrochemical protein biosensor is schematically illustrated in **Scheme 1**. It is based on two rationally designed hairpins, one of which (Hp1) is labeled with a thiol group at 3′-terminus and can be immobilized onto the Au electrode by a strong Au-S interaction. Another hairpin (Hp2) is designed with two appended single-stranded tails on both ends, which can hybridize with the recognition element-conjugated DNA strands to construct a protein responsive switch of Hp2 scaffold. The Hp1 and Hp2 can form a kissing complex on the electrode surface through the apical loop-loop or kissing interaction of the RNA-RNA base sequences. The Hp2 is also labeled with a biotin moiety at 5′-terminus. After the kissing complex formation between the Hp2 scaffold and the Hp1, the streptavidin-labeled alkaline phosphatase (SA-ALP) can be specifically introduced on the electrode surface, which then catalyzes the conversion of

electrochemically inactive 1-naphthyl phosphate (1-NP) into an electrochemically active phenol for the generation of an electrochemical signal (Carpini et al., 2004). The further protein binding to the recognition elements linked onto the Hp2 scaffold endows the steric strain to shift the Hp2 conformation from a folded to an unfolded hairpin shape, thus disrupting the kissing complex structure for the release of Hp2 from electrode surface. Accordingly, the SA-ALP could not be conjugated onto the electrode surface, resulting into a decreased electrochemical signal. Thus, protein recognition information can be quantified based on the electrochemical signal change before and after its binding. After protein-induced kissing complex dissociation, the Hp1 immobilized electrode can be directly regenerated for the successive kissing complex formation and protein recognition.

<<Herein Scheme 1>>

3.2 Detection feasibility of the kissing complex-based biosensor toward Anti-Dig antibody.

The kissing complex formation between the immobilized Hp1 and the biotin-labeled Hp2 scaffold on the electrode is firstly explored. It could be seen from Figure 1A that the Hp1 immobilized electrode showed only a very weak electrochemical response (curve a in Figure 1A), which might be attributed to the nonspecifically adsorbed trace amounts of SA-ALP on the electrode surface. After incubation of the Hp1 immobilized electrode with the Hp2 scaffold, a distinct electrochemical oxidation signal at the potential of about 0.26 V could be obtained (curve b in Figure 1A), indicating that the SA-ALP could be effectively conjugated onto the electrode through the kissing complex formation for the generation of a prominent electrochemical response. Such kissing complex formation between the Hp1 and Hp2 has been well known to be dependent upon a 6 bp loop-loop helix that includes one GU and five GC pairs (Durand et al., 2014; Chovelon et al., 2016). It could be also seen from Figure 1B that the kissing complex could not effectively occur in the cases that one or two G-G mismatches were included in the

loop-loop helix. After kissing complex formation on the electrode surface, the modified electrode was then used to explore the detection toward Anti-Dig antibody. The addition of Anti-Dig antibody could induce an obvious current decrease (curve d in Figure 1A). But the blank solution induced almost no current decrease (curve c in Figure 1A), indicating the detection feasibility of the fabricated kissing complex-based electrochemical biosensor toward Anti-Dig antibody. The kissing complex-based electrochemical biosensor for Anti-Dig antibody detection could be also characterized by cyclic voltammetric and amperometric methods (Figure S1). The detection mechanism can be attributed to the concurrent binding of Anti-Dig antibody with its two adjacent recognition elements (Dig) onto the Hp2 scaffold, which endows the steric strain to open the Hp2 stem and disrupt the kissing complex for the current decrease. To verify this point, different Hp2 scaffolds were also designed that contained only one or no Dig recognition element. In these cases, no evident current decrease could be observed (Figure 1C). This supported the interaction mechanism that the simultaneous binding of Anti-Dig antibody with its two Dig elements induced the cascade dissociation of kissing complex for the observed current decrease. The kissing complex formation and protein recognition on the electrode surface was also verified by EIS experiments (Figure 1D). After kissing complex formation between the Hp1 and Hp2 scaffold on the electrode surface, the electrochemical impedance increased obviously compared with that of Hp1 and MCH immobilized electrode. Instead, the following Anti-Dig antibody recognition induced an evident impedance decrease compared with that of kissing complex modified electrode. The EIS experiments further provided beneficial surports for the kissing complex formation on the electrode and the liberation of Hp2 scaffold by protein recognition. The kissing complex formation between Hp1 and Hp2 scaffold was also verified by gel electrophoresis experiments (Figure S2). The lanes 1, 2, 3, and 5 exhibited the bands for the Hp2, Dig-labeled S1, Dig-labeled S2 and Hp1, respectively. The lane 4 showed the bright band for the Hp2 scaffold constructed by Hp2, Dig-labeled S1 and

Dig-labeled S2. After kissing complex formation between Hp1 and Hp2 scaffold, a new bright band with obviously decreased migration shift was observed (lane 6). Furthermore, an evident brightness decay for the band of kissing complex could be seen after incubation with Anti-Dig antibody (lane 7), reflecting the kissing complex dissociation by protein binding to some extent.

<<Herein Figure 1>>

3.3 Optimization of experimental conditions

In order to achieve the best sensing performance, the corresponding experimental conditions were optimized. Firstly, the immobilization concentration of Hp1 was examined on the basis of the electrochemical response toward Anti-Dig antibody. It could be found from Figure 2A that the immobilization concentration of 1.0 μM of Hp1 could achieve the better electrochemical response than that at other concentrations. The higher immobilization concentration of Hp1 could increase the assembly density on the electrode surface, but it might restrict the kissing complex formation between the Hp1 and Hp2 scaffold owing to the steric hindrance effect, resulting into an adverse electrochemical response toward Anti-Dig antibody. The interaction time for the kissing complex formation between the Hp1 immobilized electrode and the Hp2 scaffold was also studied. The kissing complex formation contributes the introduction of SA-ALP on the electrode surface for the generation of electrochemical signal. It could be seen from Figure 2B that the electrochemical intensity increased with increasing incubation time and then reached almost the plateau value at 60 min. Then 60 min was chosen as the optimum time for the incubation of Hp2 scaffold with the immobilized Hp1. Also, the response time for the Anti-Dig antibody recognition was investigated (Figure 2C). The protein-induced dissociation of kissing complex can result into a decrease of observed electrochemical signal. It could be found that the electrochemical intensity decreased with the incubation time of Anti-Dig antibody. At about 45 min of incubation, the

electrochemical intensity almost reached the minimum value. Thus the reaction time for the Anti-Dig antibody with the kissing complex modified electrode was determined as 45 min. The effect of pH value on the electrochemical response toward Anti-Dig antibody was also studied (Figure S3). A maximum response could be achieved at pH 7.4 compared with that at other studied pH values.

<<Herein Figure 2>>

3.4 Detection performance toward Anti-Dig antibody

Under the optimized experimental conditions, the detection performance of the kissing complex-based electrochemical biosensor was investigated by using a series of different concentrations of Anti-Dig antibody ranging from 0 to 0.4 μg/mL. As shown in Figure 3A, the dynamically decreased DPV peak current with the increasing Anti-Dig antibody concentration indicated that the dissociation of kissing complex for current decrease was highly dependent on the Anti-Dig antibody concentration. The calibration plot between the DPV peak current decrease ($\Delta I = I_o - I$; the I_o and I represent the electrochemical response in the absence or presence of Anti-Dig antibody, respectively) and the Anti-Dig antibody concentration is shown in Figure 3B. A good linear relationship between the ΔI and the Anti-Dig antibody concentration ranging from 1 to 40 ng/mL could be obtained with a correlation coefficient of about 0.9947 (inset in Figure 3B). The detection limit, which was defined as 3 times the standard deviation of the background value, was approximately 1 ng/mL. Furthermore, the reproducibility of the kissing complex-based electrochemical biosensor was investigated. The relative standard deviations (RSDs) toward two different Anti-Dig antibody concentrations of 10 and 100 ng/mL were obtained as 7% and 6.2%, respectively, based on five repetitive measurements, indicating an acceptable reproducibility for protein detection. The selectivity of current kissing complex-based electrochemical biosensor toward Anti-Dig antibody detection was also studied by using other proteins including thrombin, IgG and AFP (Figure 3C). It could be found that these

proteins except Anti-Dig antibody could not induce evident DPV peak current decrease, indicating the selective detection toward Anti-Dig antibody by current kissing complex-based electrochemical biosensor. Another striking advantage for current kissing complex-based electrochemical biosensor was that the Hp1 immobilized electrode could be readily regenerated after the protein-induced dissociation of kissing complex. Thus the Hp1 electrode could be reused for further kissing complex formation and protein recognition. Such regeneration experiment can avoid the relatively harsh conditions required for most nucleic acid-based biosensors. It could be found from Figure 3D that the biosensor could be regenerated at least three times. The regeneration performance might be further improved to some extent by using dual-thiolated Hp1 to enhance its immobilization and stem-loop stucture stability. Also, the Hp1 modified electrode could be used for kissing complex formation and Anti-Dig antibody recognition after its storage in the refrigerator at 4 °C for one week. The electrochemical response could remain about 90.7% of its intial response toward 0.4 μg/mL Anti-Dig antibody based on five independent experiments, demonstrating a relatively good stability of the Hp1 modified electrode for protein detection.

<<Herein Figure 3>>

3.5 Detection versatility of the kissing complex-based electrochemical biosensor

The thrombin is chosen as another protein target to demonstrate the detection universality of current kissing complex-based electrochemical biosensor (Yang et al., 2017; Li et al., 2012). The schematic illustration of the fabricated kissing complex-based electrochemical thrombin biosensor is shown in Figure 4A. In this case, the protein recognition elements conjugated into the synthesized strands of S1 and S2 were replaced by two respective aptamer sequences of thrombin. Then, the obtained responsive Hp2 scaffold can be linked onto the electrode surface by kissing complex interaction with the immobilized Hp1. In the presence of target thrombin, it can

simultaneously bind with the two aptamer sequences to open the Hp2 stem, accompanied with the dissociation of kissing complex for the current decrease. The detection feasibility toward thrombin was demonstrated in Figure 4B. Again, a large electrochemical response could be observed after the kissing complex formation between the Hp2 scaffold and the Hp1 on the electrode (curve a in Figure 4B). Then, the addition of thrombin induced an evident DPV peak current decrease (curve b in Figure 4B), which could be attributed to the thrombin binding-induced dissociation of kissing complex. Also, almost no signal change could be observed for the blank solution compared with that of kissing complex modified electrode (curve c in Figure 4B), indicating the detection feasibility of the fabricated kissing complex-based electrochemical biosensor toward thrombin. To further verify if the concurrent binding of two aptamers with thrombin contributed the current decrease, the control experiments were also conducted and shown in Figure 4C. Almost no electrochemical signal decrease could be observed when no aptamers were included. Also whether in the case of only aptamer 1 or aptamer 2 were introduced, the electrochemical signal was only very slightly decreased, indicating that the single recognition of aptamer toward thrombin could not endow an effective steric strain to open the Hp2 stem and dissociate the kissing complex. An evident current decrease could be only obtained in the coexistence of aptamer 1 and 2. This strongly verified that the synchronous interaction of two aptamers with the thrombin changed the Hp2 structure for the cascade dissociation of kissing complex. Furthermore, other proteins including IgG, Anti-Dig antibody and AFP could induce almost no current response, indicating a good selectivity toward thrombin detection (Figure 4D). The detection performance of the fabricated kissing complex-based electrochemical biosensor toward thrombin was also investigated (Figure 4E). The DPV peak current decreased dynamically with the increase of thrombin concentration. The calibration plot between the DPV peak current decrease (ΔI) and the thrombin concentration is shown in Figure 4F. A good linear relationship between the ΔI and the thrombin concentration

ranging from 10 pM to 0.2 nM could be obtained (inset in Figure 4F) with a correlation coefficient of about 0.9917. The experimental detection limit toward thrombin was about 10 pM, which was superior or comparable with that of the reported methods (Table S2). The relative standard deviations (RSDs) toward three different concentrations of thrombin including 50 pM, 0.2 nM and 10 nM were obtained as 7.9%, 5.8% and 6.4%, respectively, based on five repetitive experiments, suggesting a relatively good reproducibility for thrombin detection. The fabricated kissing complex-based electrochemical biosensor could be also regenerated for thrombin detection for at least three times (Figure 4G).

<<Herein Figure 4>>

3.6 The applicability of the fabricated kissing complex-based electrochemical biosensor in serum samples.

In order to verify the applicative feasibility of the fabricated kissing complex-based electrochemical biosensor in relatively complex biological sample, the electrochemical detection in the diluted serum samples was conducted. The electrochemical signal in the diluted serum was almost the same with that in the blank buffer (data no shown), demonstrating no measured proteins (Anti-Dig antibody or thrombin) in the diluted serum samples. The thrombin is known to be absent in serum of healthy subjects (Shuman and Majerus). The further standard addition experiments showed that the electrochemical responses in the diluted serum sample for both spiked proteins were almost comparable with that in the buffer systems (Figure S4). Also the electrochemical response increased with the increasing concentration of the spiked proteins in the diluted serum samples. The detection results for recovery experiments were also shown in Table S3. The recoveries were obtained from about 94% to 109%, suggesting the potential for protein assays in relatively complex biological matrix.

4. Conclusion

In summary, an allosteric kissing complex-based electrochemical biosensor for sensitive, regenerative and versatile detection of proteins was well developed. It took full advantage of the protein binding-induced cascade dissociation of kissing complex for protein quantification. The detection universality was demonstrated by using two proteins including Anti-Dig antibody and thrombin with the detection limits of about 1 ng/mL and 10 pM, respectively. The biosensor interface could be readily regenerated for further kissing complex formation and protein recognition, eliminating the relatively harsh conditions required for some conventional nucleic acid-based biosensors. The current biosensor was mainly committed for the detection toward multivalent proteins. It might be extended for the detection of monovalent proteins by employing the same recognition element against a monvalent protein on both strands of S1 and S2. Finally, the biosensor design should be easily extended for the integration with the kinds of detecting platforms. Thus, it may hold great potential for the sensitive biosensor fabrication served for the applications in bioanalysis, disease diagnostics, and clinical biomedicine.

Acknowledgements

This work was funded by the National Natural Science Foundation of China (No. 21475072), the Natural Science Foundation of Shandong Province of China (Nos. JQ201704, ZR2015JL007, ZR2014BM019) and the Key Research and Development Program of Shandong Province of China (2016GSF201208).

References

Bakalova, R., Zhelev, Z., Ohba, H., Baba, Y., 2005. J. Am. Chem. Soc. 127, 9328–9329.

Burbulis, I., Yamaguchi, K., Gordon, A., Carlson, R., Brent, R., 2005. Nat. Methods 2, 31–37.

Cao, Y., Zhu, S., Yu, J., Zhu, X., Yin, Y., Li, G., 2012. Anal. Chem. 84, 4314-4320.

Carpini, G., Lucarelli, F., Marrazza, G., Mascini, M., 2004. Biosens. Bioelectron. 20, 167-175.

Chen, X., Zhou, G., Song, P., Wang, J., Gao, J., Lu, J., Fan, C., Zuo, X., 2014. Anal. Chem. 86, 7337-7342.

Chikkaveeraiah, B. V., Bhirde, A. A., Morgan, N. Y., Eden, H. S., Chen, X., 2012. ACS Nano 6, 6546-6561.

Chovelon, B., Durand, G., Dausse, E., Toulmé, J. J., Faure, P., Peyrin, E., Ravelet, C., 2016. Anal. Chem. 88, 2570-2575.

Durand, G., Lisi, S., Ravelet, C., Dausse, E., Peyrin, E., Toulmé, J. J., 2014. Angew. Chem. Int. Ed. 53, 6942-6945.

Fredriksson, S., Gullberg, M., Jarvius, J., Olsson, C., Pietras, K., Gústafsdóttir, S. M., Ostman, A., Landegren, U., 2002. Nat. Biotechnol. 20, 473-477.

Han, X. X., Jia, H. Y., Wang, Y. F., Lu, Z. C., Wang, C. X., Xu, W. Q., Zhao, B., Ozaki, Y., 2008. Anal. Chem. 80, 2799-2804.

Hanash, S. M., Pitteri, S. J., Faca, V. M., 2008. Nature 452, 571-579.

Hu, J., Wang, T., Kim, J., Shannon, C., Easley, C. J., 2012. J. Am. Chem. Soc. 134, 7066-7072.

Jameson, D. M., Ross, J. A., 2010. Chem. Rev. 110, 2685-2708.

Jung, C., Ellington, A. D., 2014. Acc. Chem. Res. 47, 1825-1835.

Kosaka, P. M., Pini, V., Ruz, J. J., Silva, R. A. d., González, M. U., Ramos, D., Calleja, M., Tamayo, J., 2014. Nat. Nanotechnol. 9, 1047-1053.

Lai, S., Wang, S., Luo, J., Lee, L. J., Yang, S. T., Madou, M. J., 2004. Anal. Chem. 76, 1832-1837.

Li, C., Li, X., Wei, L., Liu, M., Chen, Y., Li, G., 2015. Chem. Sci. 6, 4311-4317.

Li, F., Zhang, H., Lai, C., Li, X. F., Le, X. C., 2012. Angew. Chem., Int. Ed. 51,

9317-9320.

Li, J., Green, A. A., Yan, H., Fan, C., 2017. Nat. Chem. 9, 1056-1067.

Li, J., Zhong, X., Zhang, H., Le, X. C., Zhu, J. J., 2012. Anal. Chem. 84, 5170-5174.

Liu, S., Liu, T., Wang, L., 2015a. Chem. Commun. 51, 176-179.

Liu, S., Cheng, C., Gong, H., Wang, L., 2015b. Chem. Commun. 51, 7364-7367.

Mahshid, S. S., Camiré, S., Ricci, F., Vallée-Bélisle, A., 2015. J. Am. Chem. Soc. 137, 15596−15599.

Rica, R. d. l., Stevens, M. M., 2012. Nat. Nanotechnol. 7, 821-824.

Rifai, N., Gillette, M. A., Carr, S. A., 2006. Nat. Biotechnol. 24, 971-983.

Ronkainen, N. J., Halsall, H. B., Heineman, W. R., 2010. Chem. Soc. Rev. 39, 1747-1763.

Shuman, M. A., Majerus, P. W., 1976, J. Clin. Invest. 58, 1249-1258.

Tang, Z., Ma, Z., 2017. Biosens. Bioelectron. 98, 100-112.

Vallée-Bélisle, A., Ricci, F., Uzawa, T., Xia, F., Plaxco, K. W., 2012. J. Am. Chem. Soc. 134, 15197-15200.

Wang, H. B., Zhang, H. D., Chen, Y., Liu, Y. M., 2015. Biosens. Bioelectron. 74, 581-586.

Wang, Q., Jiang, B., Xu, J., Xie, J., Xiang, Y., Yuan, R., Chai, Y., 2013. Biosens. Bioelectron. 43, 19-24.

Wu, Z., Wang, H., Guo, M., Tang, L. J., Jiang, J. H., 2011. Anal. Chem. 83, 3104-3111.

Wu, Z., Zhen, Z., Jiang, J. H., Shen, G. L., Yu, R. Q., 2009. J. Am. Chem. Soc. 131, 12325-12332.

Xiao, Y., Lubin, A. A., Heeger, A. J., Plaxo, K. W., 2005. Angew. Chem., Int. Ed. 44, 5456–5459.

Yang, J., Dou, B., Yuan, R., Xiang, Y., 2017. Anal. Chem. 89, 5138-5143.

Yang, Z. H., Zhuo, Y., Yuan, R., Chai, Y. Q., 2016. Anal. Chem. 88, 5189–5196.

Yetisen, A. K., Akram, M. S., Lowe, C. R., 2013. Lab Chip 13, 2210-2251.

Zhang, H., Li, F., Dever, B., Li, X. F., Le, X. C., 2013. Chem. Rev. 113, 2812–2841.

Zhang, K., Wang, K., Zhu, X., Xie, M., 2016. Biosens. Bioelectron. 78, 154-159.

Zhang, L., Zhang, K., Liu, G., Liu, M., Liu, Y., Li, J., 2015. Anal. Chem. 87, 5677-5682.

Zhang, Y. L., Huang, Y., Jiang, J. H., Shen, G. L., Yu, R. Q., 2007. J. Am. Chem. Soc. 129, 15448-15449.

Figure Captions

Scheme 1. Schematic illustration of the allosteric kissing complex-based electrochemical protein biosensing.

Figure 1. (A) The electrochemical responses for Hp1 immobilized electrode (a), kissing complex modified electrode (b), the detection toward 0 (c) and 0.4 μg/mL (d) Anti-Dig antibody. (B) DPV peak current increase after the formation of matched or mismatched kissing complex on the electrode surface. The Hp1 and Hp2 scaffold can form a 6 bp loop-loop helix that includes one GU and five GC pairs. One or two mismatched C bases were also introduced in the loop region of Hp1 as a comparison. (C) DPV peak current decrease toward detection of 0.4 μg/mL Anti-Dig antibody by using Hp2 scaffold containing two, one or no Dig elements. (D) EIS responses recorded in 10 mM $Fe(CN)_6^{3-/4-}$ and 1 M KCl solution for the different modified electrodes. The curves were obtained for bare gold electrode (a), the Hp1 and MCH immobilized (b), recognized by Hp2 scaffold (c), and after incubation with 0.4 μg/mL Anti-Dig antibody (d). The error bars were obtained based on at least three repetitive experiments.

Figure 2. (A) Optimization of Hp1 immobilization concentration. The used Hp1 concentrations were 0.1, 0.5, 1.0, 2.0 and 5.0 μM, respectively. The Y-axis indicates the DPV peak current decrease after incubation of 0.4 μg/mL Anti-Dig antibody. (B) Time dependency of the kissing complex formation on the electrode surface. (C) Time responses of the fabricated kissing complex-based electrochemical biosensor toward 0.4 μg/mL Anti-Dig antibody. Each error bar was obtained based on at least three repetitive experiments.

Figure 3. (A) DPV responses corresponding to the analysis of different concentrations of Anti-Dig antibody. The used Anti-Dig antibody concentrations were: a, 0 ng/mL; b, 1 ng/mL; c, 4 ng/mL; d, 10 ng/mL; e, 20 ng/mL; f, 40 ng/mL; g, 100 ng/mL; h, 200 ng/mL; i, 0.4 μg/mL. (B) Calibration plot between the DPV peak current decrease ($\Delta I = I_o - I$; the I_o and I

represent the electrochemical response in the absence or presence of Anti-Dig antibody, respectively) and the Anti-Dig antibody concentration. Inset shows the corresponding linear relationship. (C) Selectivity test toward the Anti-Dig antibody and other non-specific proteins including thrombin, AFP and IgG. The concentrations for the Anti-Dig antibody, thrombin, AFP and IgG were 0.4 μg/mL, 10 nM, 1 μg/mL and 1 μg/mL, respectively. (D) Regeneration experiments for the kissing complex-based electrochemical biosensor toward the detection of 0.4 μg/mL Anti-Dig antibody. After protein recognition, the Hp1 modified electrode could be directly reused for the successive kissing complex formation and protein detection. The error bars were obtained based on at least three repetitive experiments.

Figure 4. (A) Schematic illustration of the kissing complex-based electrochemical biosensor for thrombin detection. (B) Electrochemical responses for the kissing complex modified electrode (a), toward the detection of 10 nM thrombin (b) or blank solution (c). (C) DPV peak current decrease toward 10 nM thrombin by using various Hp2 scaffolds that contains different aptamer elements. (D) Selectivity test toward 10 nM thrombin and other non-specific proteins including IgG, Anti-Dig antibody and AFP with the same concentration of 1 μg/mL. (E) DPV responses corresponding to the analysis of different concentrations of thrombin. The used thrombin concentrations were: a, 0 pM; b, 10 pM; c, 20 pM; d, 50 pM; e, 0.1 nM; f, 0.2 nM; g, 0.5 nM; h, 1 nM; i, 5 nM; j, 10 nM. (F) Calibration plot between the DPV peak current decrease and the thrombin concentration. Inset shows the linear relationship. (G) Regeneration experiments for the kissing complex-based electrochemical biosensor toward the detection of 10 nM thrombin. The error bars were obtained based on at least three repetitive experiments.

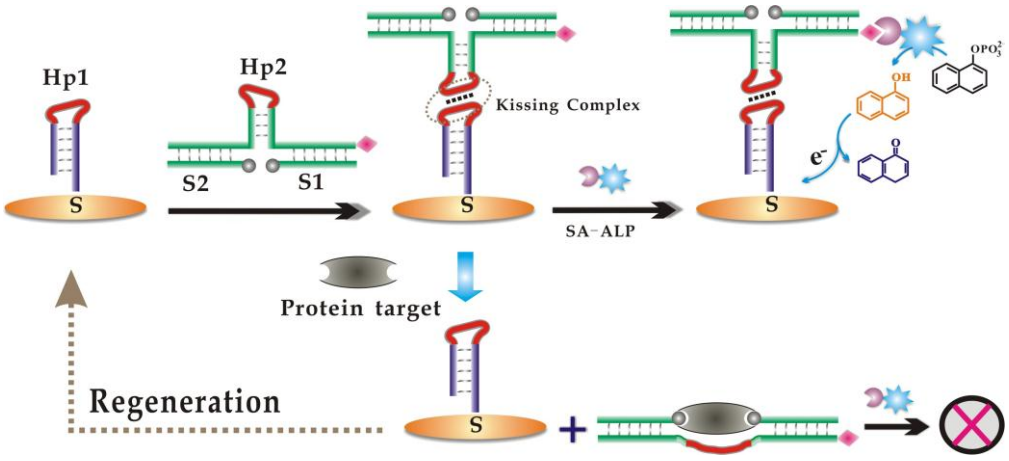

Scheme 1

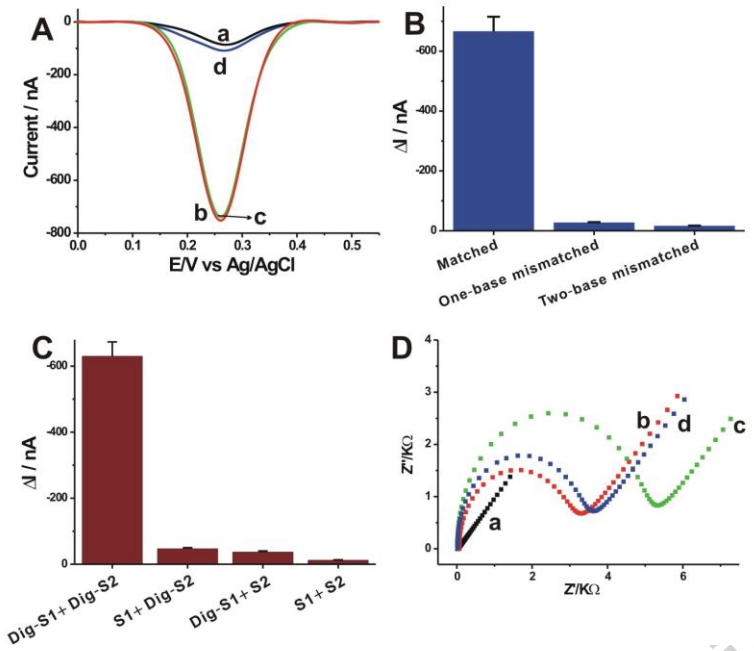

Figure 1

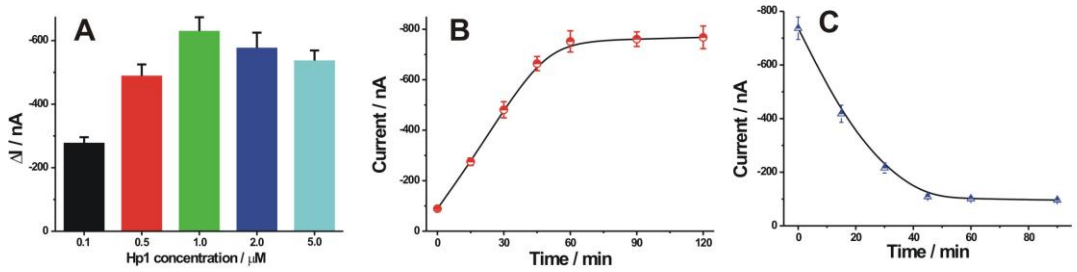

Figure 2

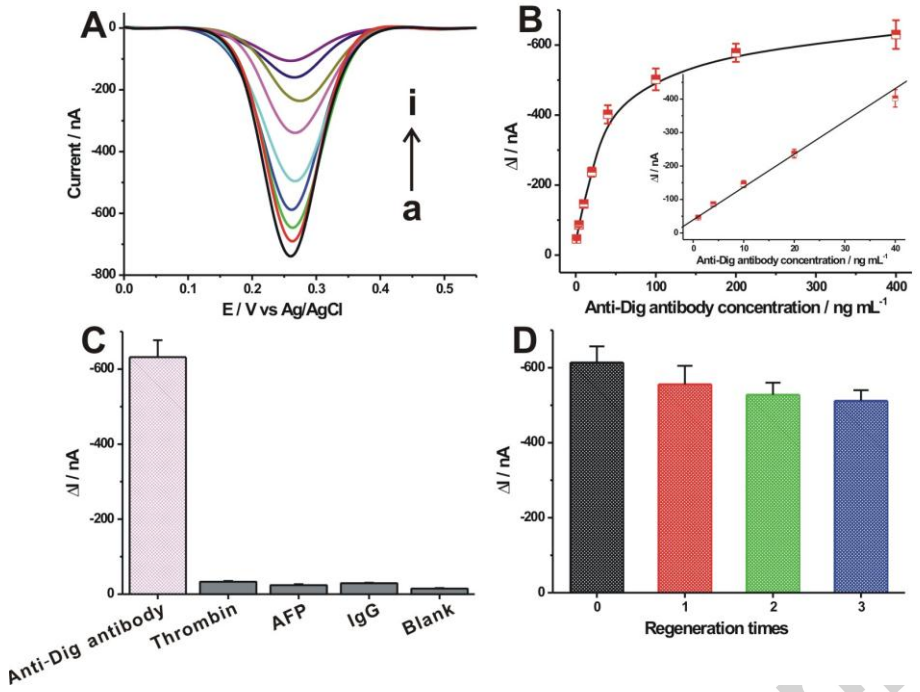

Figure 3

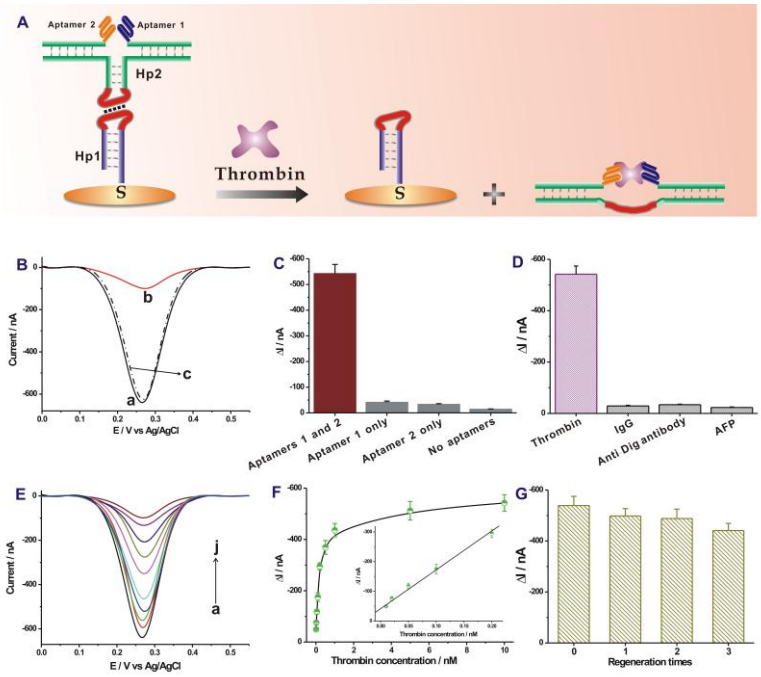

Figure 4

Highlights

- An allosteric kissing complex-based electrochemical protein biosensor was proposed.
- It takes advantage of the protein binding-induced cascade dissociation of kissing complex.
- The biosensor could be regenerated after protein recognition.
- The detection universality was demonstrated by Anti-Dig antibody and thrombin.